ELSEVIER

Dynamics of Atmospheres and Oceans
31 (2000) 193–207

dynamics of atmospheres and oceans

www.elsevier.com/locate/dynatmoce

Wave/wave interaction producing horizontal mean flows in stably stratified fluids

M. Galmiche [a,*], O. Thual [a], P. Bonneton [b]

[a] *Institut de Mécanique des Fluides de Toulouse Allée du Professeur Camille Soula, 31400 Toulouse, France*
[b] *Département de Géologie et d'Océanographie, URA CNRS 197 Université Bordeaux 1, 33405 Talence, France*

Received 23 June 1998; received in revised form 12 March 1999; accepted 23 March 1999

Abstract

We show that internal wave/wave interactions in stratified fluids are able to produce strong horizontal mean currents. A simple analytical model allows us to estimate the amplitude of the time-periodic horizontal mean flow induced by the interaction of two monochromatic waves. This model shows that in some cases, the mean flow velocity can overgo a threshold beyond which critical layers and intense energy transfers from the waves to the mean flow are expected. This prediction is confirmed by direct pseudo-spectral simulations of the Navier–Stokes equations under the Boussinesq approximation. Such interactions may help to further understand the presence of strong vertical shear observed in the final stage of stratified flows in oceans and atmospheres.

Keywords: Wave/wave interaction; Horizontal mean flows; Stratified fluids

1. Introduction

The presence of internal gravity waves is one of the main features of geophysical stratified flows. Wave fields may be generated by shear instabilities, wakes, tides, topographic effects or more generally turbulent motions in stratified regions of oceans and atmospheres.

* Corresponding author.

0377-0265/00/$ - see front matter
PII: S0377-0265(99)00033-0

Attention was already paid to wave/wave interactions in stratified media. As pointed out by Garrett and Munk (1979), an important issue is the influence of such interactions on energy spectra in the oceans. Nonlinear triadic interactions give rise to energy transfers provided that the frequencies and wavevectors of the modes involved verify the resonance condition.

Investigating the possible wave action transfers in internal wave energy spectra, McComas and Bretherton (1977) concluded that three kinds of resonant triadic interactions could take place. The most rapid process, called *induced diffusion*, involves two modes with similar wave vectors and frequencies, and a large-scale, low-frequency mode. Induced diffusion may play an important role in the shape of energy spectra at low wavenumbers. The second process, called *elastic scattering*, involves an upward propagating mode and a downward propagating mode. This process tends to balance the upward and downward energy fluxes on a time scale of order one wave period. This accounts for the often-observed vertical symmetry of wave fields in the oceans. The third process is the *parametric subharmonic instability* which transfers energy to high wavenumbers. This mechanism has a great effect on the inertial range of energy spectra and may account for the high activity of small-scale waves in stratified oceans.

From a theoretical point-of-view, Lelong and Riley (1991) studied wave–wave interactions with a multiple-scale method. They also considered triads involving a vertical vorticity mode. From an experimental point-of-view, Martin et al. (1972) have observed the excitation of several resonant triads by the propagation of a single internal wave. Teoh et al. (1997) studied the interaction between two internal wave rays in salt water and observed the production of evanescent modes in the interaction region. In this region, wave energy was accumulated but turbulent kinetic energy was locally dissipated and the mixing efficiency was weak.

Few studies have paid attention to triads involving a vertical wavevector which is actually associated with a non propagating, horizontal mean flow. However, Phillips (1968) has shown that internal gravity waves can be trapped by a vertically modulated horizontal current giving rise to the *elastic scattering* triadic interaction.

Furthermore, some studies have shown that horizontal mean flows strongly interact with internal waves. As experimentally observed by Koop (1981), internal waves propagating in a horizontal mean flow $U(z)$ can reach a critical level. This happens at an altitude z_c where the Taylor–Goldstein equation becomes singular, i.e.,

$$U(z_c) = \omega/k_1, \tag{1}$$

where ω is the angular frequency of the wave and k_1 is the horizontal wave number. Booker and Bretherton (1967) have theoretically studied energy transfers at a critical level and concluded that an acceleration of the mean flow could result at the critical altitude. The numerical simulations performed by Winters and D'Asaro (1994) have actually shown that in most cases, wave energy was not only transferred to the mean flow but also converted into turbulent motions or transferred to the reflected wave. In the present article, we show that critical layer mechanisms can be involved in wave–wave interactions and lead to a significant energy transfer from the waves to the mean flow.

Only bidimensional cases are considered in the x–z vertical plane where z is the spatial coordinate in the direction of gravity and x is the spatial coordinate in the

horizontal direction. The horizontal mean flow $U(z)$ is defined as the average of the horizontal velocity in each horizontal plane of altitude z. In Section 2, we use a simple analytical model to estimate the amplitude of the time-periodic mean flow induced by the interaction of two monochromatic waves. The modes involved are similar to those involved in the interaction described by Phillips (1968). The waves are supposed to remain unperturbed by the induced mean flow. This model shows that in some cases, the velocity of the shear flow *catalysed* by the wave/wave interaction can locally reach a value such that the critical layer condition (1) is satisfied for one of the two waves or both. Then, the shearing motion is expected to accelerate and to lose its time-periodicity. We give a simple criterium which allow us to determine whether or not such a critical level is reached.

This criterium based on simple, linear argument is confirmed in Section 3 by bidimensional direct numerical simulations of the interaction between two monochromatic internal waves. A pseudo-spectral code (Thual, 1992) is used to solve the complete, non-linear Navier–Stokes equations under the Boussinesq approximation with fully periodic boundary conditions.

2. The analytical model

2.1. Equations of motion

In this section, we propose a simple analytical model describing the evolution of the mean flow induced by the interaction of two monochromatic internal waves in a thermally stratified fluid with constant and uniform Brunt–Väïsälä frequency N. Under the Boussinesq approximation, variations of density ρ are assumed to induce buoyancy forces without affecting the inertial terms and to linearly depend of temperature T: $(\rho-\rho_0)/\rho_0=\alpha(T-T_0)$, where subscript 0 stands for a reference state and α is the expansion coefficient. Then, the equations of motion may be written in a cartesian coordinate system $(\mathbf{e}_1, \mathbf{e}_2, \mathbf{e}_3)$ as:

$$\begin{cases} \nabla\cdot\mathbf{u}=0 \\ \partial_t\mathbf{u}+(\mathbf{u}\cdot\nabla)\mathbf{u}=-\rho_0^{-1}\nabla p+\alpha g\theta\mathbf{e}_3+\nu\nabla^2 u \\ \partial_t\theta+(\mathbf{u}\cdot\nabla)\theta=-Gw+\kappa\nabla^2\theta \end{cases} \tag{2}$$

where $\mathbf{u}(x, y, z, t)=(u, v, w)$, and p are the velocity and pressure fields. Variable θ represents the temperature fluctuations from the stable, mean profile. x, y, z and t are the space and time coordinates and $\nabla=(\partial_x, \partial_y, \partial_z)$. g is the acceleration of gravity, ν is the kinematic viscosity and κ is the thermal diffusivity. G is the mean temperature vertical gradient. The Brunt-Väïsälä frequency is defined by: $N^2=\alpha gG$.

We choose fully periodic boundary conditions with periodicity L_b (the size of the periodic domain) and we will only consider bidimensional, incompressible flows. Then, the velocity field $\mathbf{u}(x, z, t)=(u(x, z, t), w(x, z, t))$ is fully described by variables: $w(x, z, t)$, the vertical velocity, and $U(z, t)$, the horizontally averaged horizontal

velocity. Component $u(x, z, t)$ is easily deduced from the resolution of the incompressibility condition $\partial_x u = -\partial_z w$ with periodic boundary conditions, knowing that

$$\langle u(x,y,z,t)\rangle^{xy} = U(z,t), \tag{3}$$

where $\langle . \rangle^{xy}$ is the horizontal average operator, i.e.,

$$\langle q(x,y,z)\rangle^{xy} = \frac{1}{L_b^2}\int_0^{L_b}\int_0^{L_b} q(x,y,z)\,\mathrm{d}x\,\mathrm{d}y.$$

for any quantity $q(x, y, z)$.

Equations for variables $w(x, z, t)$, $\theta(x, z, t)$ and $U(z, t)$ read:

$$\begin{cases} \partial_t \nabla^2 w - \nabla \wedge \left(\nabla \wedge \left[(\mathbf{u}\cdot\nabla)\mathbf{u}\right]\right)\cdot \mathbf{e}_3 = \alpha g \partial_{xx}\theta + \nu\nabla^4 w \\ \partial_t \theta + (\mathbf{u}\cdot\nabla)\theta = -Gw + \kappa\nabla^2\theta \\ \partial_t U + \partial_z\langle uw\rangle^{xy} = \nu\partial_{zz}U \end{cases} \tag{4}$$

2.2. The mean flow induced by two internal waves

Let us write the bidimensional velocity field as:

$$\underline{u} = (u,w) = (U(z,t) + u'(x,z,t),\, w'(x,z,t)), \tag{5}$$

where $U(z, t)$ is the horizontal parallel flow and $(u'(x, z, t), w'(x, z, t))$ is associated with a small-amplitude wave field. It is clear from Eq. (4) that this wave field is subject to the distortion by the mean flow. However, to a first approximation, we will consider that the waves are only weakly distorted. Also, nonlinear terms will be neglected in the equations of w and θ as well as the effect of dissipation. Then, we get the linear, non-dissipative internal wave equation:

$$\frac{\partial^2\nabla^2 w'}{\partial t^2} + N^2\frac{\partial^2 w'}{\partial x^2} = 0. \tag{6}$$

Let us consider the superposition of two monochromatic internal waves A and B:

$$\begin{cases} u' = u'_A + u'_B \\ w' = w'_A + w'_B \end{cases} \tag{7}$$

$$\begin{cases} u'_A = -(k_{3A}/k_{1A})\, w'_{0A}\cos(k_{1A}x + k_{3A}z - \omega_A t + \varphi_A) \\ w'_A = w'_{0A}\cos(k_{1A}x + k_{3A}z - \omega_A t + \varphi_A) \end{cases} \tag{8}$$

$$\begin{cases} u'_B = -(k_{3B}/k_{1B})\, w'_{0B}\cos(k_{1B}x + k_{3B}z - \omega_B t + \varphi_B) \\ w'_B = w'_{0B}\cos(k_{1B}x + k_{3B}z - \omega_B t + \varphi_B) \end{cases} \tag{9}$$

This wave field is the superposition of waves A and B with small amplitudes w'_{0A} and w'_{0B}, wave vectors $\mathbf{k}_A = (k_{1A}, k_{3A})$ and $\mathbf{k}_B = (k_{1B}, k_{3B})$, frequencies ω_A and ω_B and phase shifts φ_A and φ_B. Eq. (6) is satisfied if ω_A and ω_B verify the dispersion relation:

$$\omega_A = N\frac{k_{1A}}{\sqrt{k_{1A}^2 + k_{3A}^2}} = N\cos\beta_A \tag{10}$$

$$\omega_B = N\frac{k_{1B}}{\sqrt{k_{1B}^2 + k_{3B}^2}} = N\cos\beta_B \tag{11}$$

where β_A (respectively β_B) is the angle between $\mathbf{k}_A$ (respectively $\mathbf{k}_B$) and the horizontal direction $\mathbf{e}_1$.

We now consider the evolution equation of $U(z, t)$. This equation reads:

$$\partial_t U + \partial_z \langle u'w' \rangle^x = 0 \tag{12}$$

Thus, the wave-induced mean current is quadratic in the waves amplitude and it is straightforward that $\partial_z \langle u'w' \rangle^x \equiv 0$ unless waves A and B are such that $k_{1A} = k_{1B}$ or $k_{1A} = -k_{1B}$. In the following, we will only consider the second case and we will note $k_{1A} = k_1 > 0$ and $k_{1B} = -k_1 < 0$, the results being easily extended to the case where $k_{1A} = k_{1B}$. Then, cos $\beta_A \in [0, 1]$ and cos $\beta_B \in [-1, 0]$.

Eq. (12) reads:

$$\partial_z \langle u'w' \rangle^x = \frac{w'_{0A}w'_{0B}}{2}\left(\frac{k_{3A}^2 - k_{3B}^2}{k_1}\right)\sin\big[(k_{3A} + k_{3B})z - (\omega_A + \omega_B)t + (\varphi_A + \varphi_B)\big] \tag{13}$$

Let us choose the initial condition $U(z, 0) = 0$ for Eq. (12). This leads to the solution:

$$U(z,t) = Mk_1\frac{w'_{0A}w'_{0B}}{2N}\big[\cos(Kz - \Omega t + \phi) - \cos(Kz + \phi)\big] \tag{14}$$

where

$$M = \frac{\tan^2\beta_A - \tan^2\beta_B}{\cos\beta_A + \cos\beta_B} = \frac{\cos\beta_B - \cos\beta_A}{\cos^2\beta_A\cos^2\beta_B}, \tag{15}$$

$K = k_{3A} + k_{3B}$, $\Omega = \omega_A + \omega_B$ and $\phi = \varphi_A + \varphi_B$

2.3. Critical layer criterium

We now have the solution for the mean flow induced by the interaction of waves A and B. Now we would like to know whether this mean flow is strong enough so that

wave A or B can locally develop a critical layer. According to Eq. (1), a necessary condition for this to happen is that its amplitude overgoes one of the thresholds:

$$U_{cA} = \frac{\omega_A}{k_{1A}} \text{ or } U_{cB} = \frac{\omega_B}{k_{1B}}.$$

Thus a critical layer may appear if

$$U_M \geq \min(|U_{cA}|,|U_{cB}|), \tag{16}$$

where U_M is the maximum (positive) value that the mean flow can reach. From Eq. (14), the value of U_M is given by:

$$U_M = Mk_1 \frac{w'_{0A}w'_{0B}}{N} \tag{17}$$

We are now going to look for a criterium in terms of the dimensionless parameter

$$Q = \frac{k_1\sqrt{w'_{0A}w'_{0B}}}{N} \tag{18}$$

Using Eq. (10), Eq. (11), Eqs. (17) and (18), we can calculate U_{cA}, U_{cB} and U_M in function of Q:

$$U_{cA} = \sqrt{w'_{0A}w'_{0B}}\,\frac{\cos\beta_A}{Q} \tag{19}$$

$$U_{cB} = \sqrt{w'_{0A}w'_{0B}}\,\frac{\cos\beta_B}{Q} \tag{20}$$

$$U_M = \sqrt{w'_{0A}w'_{0B}}\,Q|M| \tag{21}$$

Then, criterion (16) can be equivalently written in terms of Q:

$$Q \geq \min(Q_A, Q_B) \tag{22}$$

where

$$Q_A = \sqrt{\left|\frac{\cos\beta_A}{M}\right|} \text{ and } Q_B = \sqrt{\left|\frac{\cos\beta_B}{M}\right|} \tag{23}$$

We see that this condition depends not only on the value of Q but also on trigonometric functions which determine the values of the thresholds. Let us use Eq. (15) to write again $Q_A Q_B$ in function of $\cos\beta_A$ and $\cos\beta_B$:

$$Q_A = \sqrt{\left|\frac{\cos\beta_A}{\cos\beta_A + \cos\beta_B}\cos^2\beta_A\cos^2\beta_B\right|} \tag{24}$$

$$Q_B = \sqrt{\left|\frac{\cos\beta_B}{\cos\beta_A + \cos\beta_B}\cos^2\beta_A\cos^2\beta_B\right|} \tag{25}$$

The values of Q_A and Q_B in function of cos β_A and cos β_B are plotted on Fig. 1. Given the values of cos β_A, cos β_B and Q, this plot allows us to determine whether or not condition (22) is verified. We see that for low values of cos β_A and cos β_B, the values of the thresholds Q_A and Q_B can be small.

One will notice that the wave–wave–mean flow interaction is spatially resonant but not temporally resonant in the general case because the frequency of the induced mean flow does not automatically verify the dispersion relation. It is only the case when $\Omega = 0$ but this requires that cos $\beta_B = -\cos\ \beta_A$ and then $\partial_z \langle u'w' \rangle^x = 0$ (see Eq. (13)) and no mean flow is produced. This means that an anisotropy (or asymmetry) of the wave field is needed to give rise to a horizontal mean flow.

Notice that planes cos $\beta_A = 0$ and cos $\beta_B = 0$ do not have to be taken into account because in that case, waves have actually to be considered as non-propagative vertical shearing modes. However, an interesting result is that the value of the critical threshold for wave A (respectively wave B) is very low when cos β_A (respectively wave cos β_A) is close to zero. This happens when one of the two waves propagates almost vertically with almost horizontal phase planes. In this case, we thus expect that a critical level will

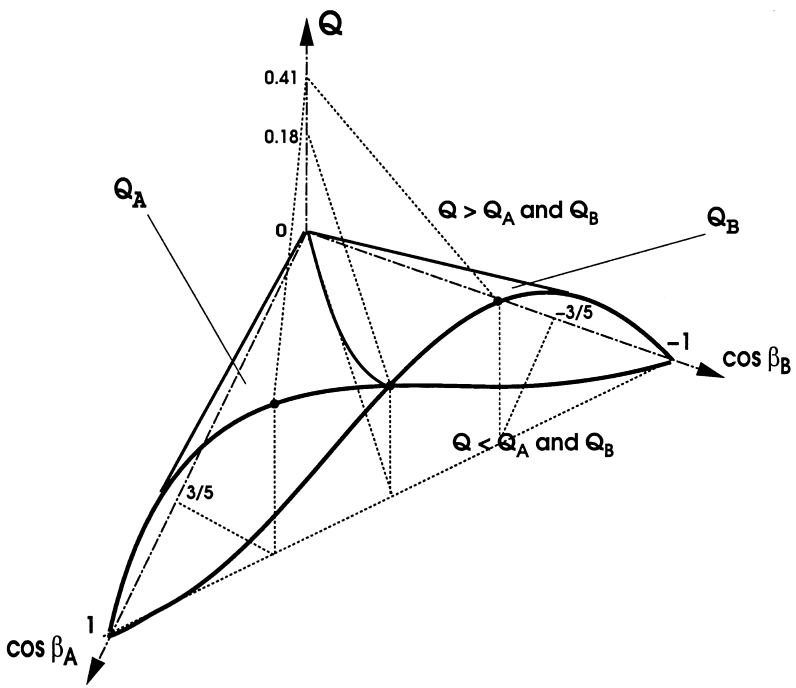

Fig. 1. Thresholds Q_A and Q_B as a function of cos β_A and cos β_B. Given the values of cos β_A, cos β_B and Q, this plot allows us to determine whether or not the mean flow induced by the wave–wave interaction can reach the critical level of wave A, wave B or both. Q_A (respectively Q_B) is maximum for cos $\beta_A = 3/5$ (respectively cos $\beta_B = -3/5$). The maximum value of Q_A and Q_B is 0.41. For cos $\beta_A = 0.5$ and cos $\beta_B = -0.5$, we have $Q_A = Q_B = 0.18$.

be reached for almost any value of Q. This may be a scenario for energy transfers from almost horizontal wavy motions to purely horizontal mean currents.

We conclude that the interaction of two internal gravity waves with amplitudes w'_{0A} and w'_{0A} and wavevectors $\mathbf{k}_A = (k_{1A}, k_{3A})$ and $\mathbf{k}_B = (k_{1B}, k_{3B})$ are able to produce a horizontal mean flow if $|k_{1A}| = |k_{1B}|$ and $|k_{3A}| \neq |k_{3B}|$. Furthermore, critical layers and intense energy transfers from the waves to the mean flow may occur if the dimensionless parameter $Q = k_1\sqrt{w'_{0A}w'_{0B}}/N$ (where N is the Brunt–Väïsälä frequency of the stratification) is such that

$$Q \geq \min(Q_A, Q_B),$$

where Q_A and Q_B depend on the orientation of the wave vectors and are given by Eqs. (24) and (24). However, our model does not allow us to predict the evolution of the flow once a critical level is reached. Then, the complete set of nonlinear equations has to be considered.

3. Direct numerical simulation

3.1. Methodology

In order to check that the conclusions of Section 2 are relevant, we performed direct numerical simulations of the interaction between two monochromatic internal gravity waves. The complete set of nonlinear, dissipative Eq. (4) was solved by a pseudo-spectral code (Thual, 1992). The boundary conditions are fully periodic and the spatial resolution is 64×64. All the variables are expressed in the Fourier space and nonlinear terms are calculated in the physical space. We use a second-order *slaved-frog* temporal scheme (see Frisch et al., 1986).

The flow evolves in a periodic square box of size L_b with no external forcing, the initial condition being the superposition of two monochromatic internal waves A and B with horizontal wavenumbers $k_{1A} = 2\pi/L_b$ and $k_{1B} = -2\pi/L_b$ (see Fig. 2). Obviously, nonlinear interactions and dissipation are now allowed so that the velocity field is not expected to keep the simple expression (7) all along the simulation. The initial condition is chosen such that:

$$w'_{0A} = w'_{0B} = w'_0,$$

the initial amplitude of the waves,

$$k_{1A} = -k_{1B} = k_1 = 2\pi/L_b,$$

$$k_{3A} = 2\pi/L_b \text{ and } k_{3B} = -4\pi/L_b,$$

$$\varphi_A = 0 \text{ and } \varphi_B = 0.$$

So that:

$$\cos\beta_A = 1/\sqrt{2} \text{ and } \cos\beta_B = -1/\sqrt{5}.$$

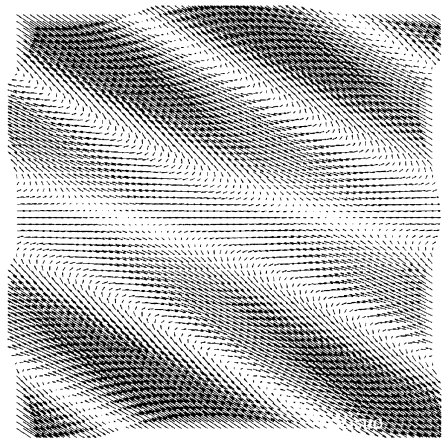

Fig. 2. Initial velocity field (arrows) in a vertical plane for the numerical simulations: superposition of two monochromatic internal waves with no vertical mean shear.

And

$$Q_A = 0.247 \text{ and } Q_B = 0.197$$

The simulations are fully defined by the values of:

$$Re = w_0' L_b / \nu,$$

the initial Reynolds number;

$$P = \nu / K$$

the Prandtl number;

$$Q = k_1 w_0' / N.$$

The resolution of 64^2 allows: Re = 833, $P = 1$.Two simulations were performed: (i) Sub-critical simulation (Simulation I): $Q = 0.13 < \min(Q_A, Q_B)$, (ii) Over-critical simulation (Simulation II): $Q = 0.31 > \max(Q_A, Q_B)$.In order highlight the global evolution of the mean current, we plotted its total energy within the box against time (see Fig. 3):

$$E_{sh}(t) = \frac{1}{L_b} \int_0^{L_b} \frac{1}{2} U^2(z,t) \mathrm{d}z$$

3.2. Sub-critical simulation

In the sub-critical simulation (Simulation I), we observe a time-periodic mean current energy (see Fig. 3), which is consistent with the conclusions of Section 2.

As can be seen on the velocity fields shown on Fig. 4, the waves are not significantly perturbed by the induced mean flow but are slowly dissipated along the simulation. No energy is transferred to smaller structures which is typical of a weak interaction.

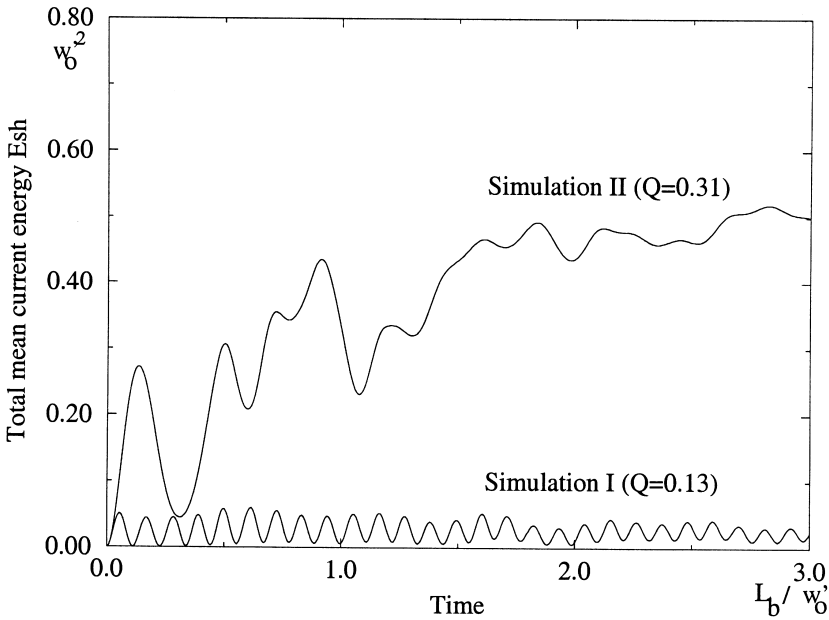

Fig. 3. Evolution of the total mean current energy in Simulations I (sub-critical) and II (over-critical). The velocity scale is w'_0. The time scale is L_b / w'_0. In Simulation I, the mean current remains time-periodic whereas in Simulation II, it loses its periodicity and finally dominates the flow.

Nevertheless, we notice that the mean current energy oscillates around a mean value which slowly increases along the simulation and does not reach zero anymore along its

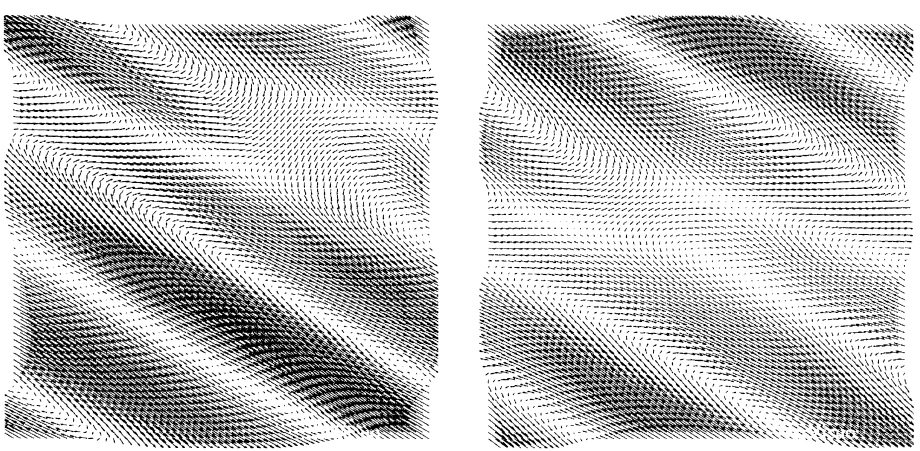

Fig. 4. Simulation of wave/wave interaction in the sub-critical case ($Q = 0.13 < \min(Q_A, Q_B)$). Velocity fields (arrows) in a vertical plane at $t = L_b / w'_0$ (left) and $t = 2L_b / w'_0$ (right). The waves are not significantly perturbed by the induced time-periodic vertical mean shear.

oscillations. This may be explained by the effect of dissipation which dissipates the wavy motions faster than the larger-scale mean flow. It is also possible that a weak nonlinearity rises in this sub-critical simulation and participates to this slow drift.

3.3. Over-critical simulation

In the over-critical simulation, it is found that the mean current produced by the wave–wave interaction rapidly loses its periodicity as evident on Fig. 3. Both waves are strongly affected by the presence of the induced mean shear and small structures are produced, which is typical of a strong nonlinear wave–shear interaction (see Fig. 5, left). After less than one time unit L_b/w'_0, a strong energy transfer is observed from the waves to the mean flow. This energy transfer seems to happen on a time scale a little slower than the waves time scale. Thus, some oscillations are still observed on Fig. 3 even after the threshold is reached. At the end of the simulation, the mean current totally dominates the flow and the remaining wavy motions are weak (see Fig. 5, right).

Thus, it is confirmed that the evolution of the mean flow is radically different when the critical layer criterium derived in Section 2 is satisfied. In addition, direct numerical simulation allows us to observe that the energy transfer is not localized in altitude as one would expect from a critical-level mechanism. Even if the criterium we derived with simple arguments seems to be relevant, this leads us to study in the last section how nonlinearity affects the energy transfer scenario described in Section 2.

3.4. Effect of nonlinearity

In order to show that the intense mean flow production observed in the over-critical simulation is not due to a simple wave instability but to the wave–mean flow

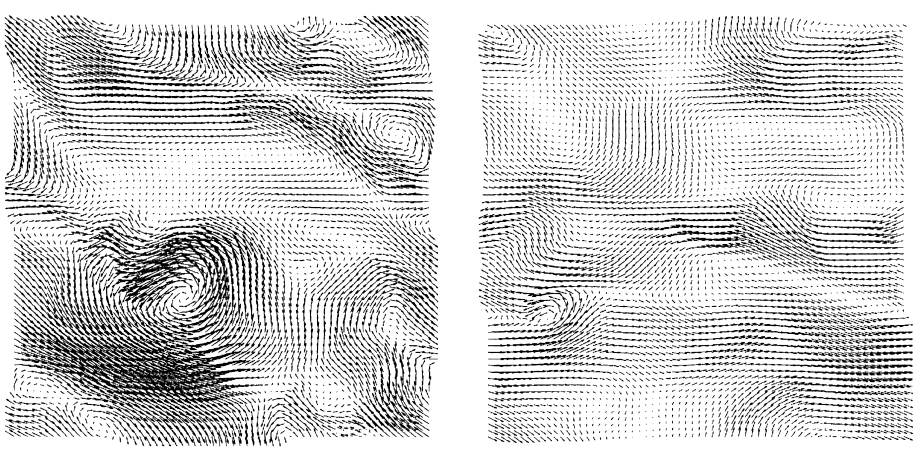

Fig. 5. Simulation of wave/wave interaction in the over-critical case ($Q = 0.31 > \max(Q_A, Q_B)$). Velocity fields (arrows) in a vertical plane at $t = L_b / w'_0$ (left) and $t = 2L_b / w'_0$ (right). The induced vertical mean shear loses its time-periodicity and dominates the flow at the end of the simulation.

interaction, we have performed the same simulation ignoring the retroaction of the mean flow onto the wave field (Simulation III). The new set of equations is:

$$\begin{cases} \partial_t \nabla^2 w' - \nabla \wedge \left(\nabla \wedge \left[(\mathbf{u}' \cdot \nabla) u' \right] \right) \cdot \mathbf{e}_3 = \alpha g \partial_{xx} \theta + \nu \nabla^4 w' \\ \partial_t \theta + (\mathbf{u}' \cdot \nabla) \theta = -G w' + \kappa \nabla^2 \theta \end{cases} \tag{26}$$

where $\mathbf{u}' = (u', w')$ is deduced from the resolution of the incompressibility condition $\partial_x u' = -\partial_z w'$ with periodic boundary conditions, specifying that

$$\langle u(x, y, z, t) \rangle^{xy} = 0. \tag{27}$$

Eq. (26) is then uncoupled from the mean flow equation:

$$\partial_t U + \partial_z \langle u' w' \rangle^{xy} = \nu \partial_{zz} U \tag{28}$$

All the parameters defining the simulation are the same as for Simulation II. The evolution of the total mean current energy is shown on Fig. 6. The velocity field $\mathbf{u} = U\mathbf{e}_1 + \mathbf{u}'$ in a vertical section is shown on Fig. 7 at $t = L_b/w'_0$ and $t = 2L_b/w'_0$.

In this simulation a roughly time-periodic mean flow is produced until $t \simeq L_b/w'_0$ (see Fig. 6). After this time, the waves become unstable (see Fig. 7, left) but the mean flow energy starts decreasing and is weak at the end of the simulation (see Figs. 6 and 7, right).

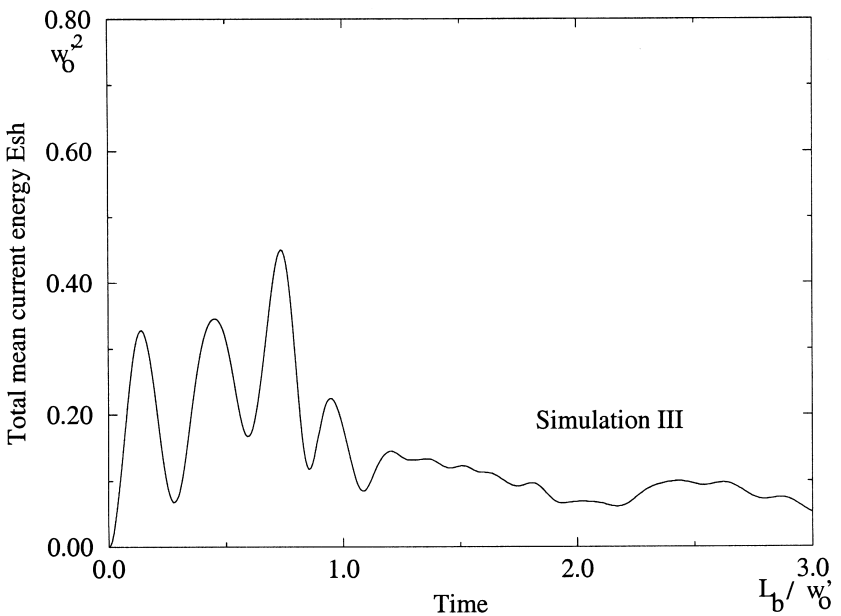

Fig. 6. Evolution of the total mean current energy in Simulation III (over-critical, with no retroaction of the mean shear on the wave field). The velocity scale is w'_0. The time scale is L_b / w'_0. At the end of the simulation, the induced mean flow is much weaker than in Simulation II.

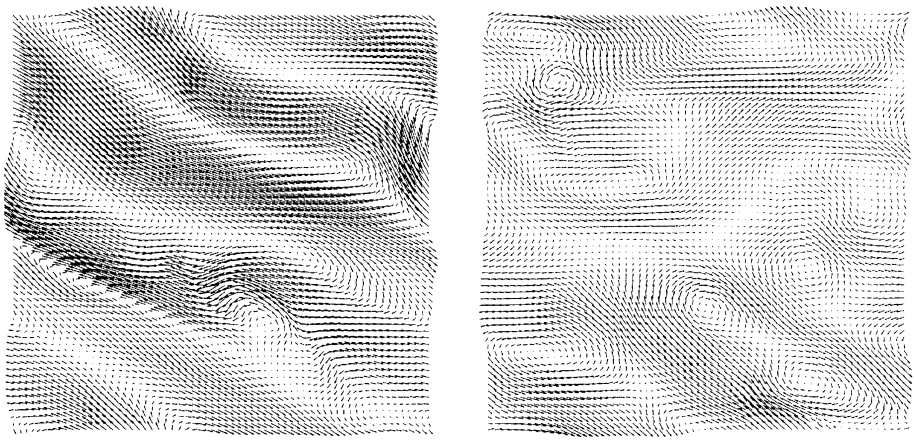

Fig. 7. Simulation of wave/wave interaction in the over-critical case with no retroaction of the mean shear on the wave field. Velocity fields (arrows) in a vertical plane at $t = L_b / w'_0$ (left) and $t = 2L_b / w'_0$ (right). The waves are unstable but the remaining mean flow is weak.

This result clearly shows that the strong acceleration of the mean current observed in Simulation II was due to the interaction of the waves with the induced mean flow as conjectured in Section 2, even if no spatially localized critical layer was detected. The wave instability observed in Simulation III may also be involved in Simulation II but this instability does not induce any significant acceleration of the horizontal mean current as shown by Simulation III and wave–mean flow interaction seems to be the dominant energy transfer mechanism from the waves to the mean flow.

4. Conclusion

We have proposed a simple 2D-analytical model describing the evolution of the horizontal mean flow induced by the superposition of two monochromatic internal gravity waves in a stratified fluid with constant and uniform Brunt-Väïsälä frequency N. In this model, waves were assumed to have small amplitudes and to remain unaffected by the induced mean flow. Nonlinear effects were neglected as well as dissipation. It was found that a time-periodic mean flow could be produced if wavenumbers $\mathbf{k}_A = (k_{1A}, k_{3A})$ and $\mathbf{k}_B = (k_{1B}, k_{3B})$ were such that $|k_{1A}| = |k_{1B}|$ and $|k_{3A}| \neq |k_{3B}|$. In addition we have found that the mean flow could either remain time-periodic (sub-critical case) or overgo a threshold beyond which a critical layer phenomenum and energy transfers from the waves to the mean flow were expected. We found that such a threshold was reached when the dimensionless parameter $Q = k_1 \sqrt{w'_{0A} w'_{0B}} / N$ (where $k_1 = |k_{1A}| = |k_{1B}|$ and w'_{0A} and w'_{0B} are the amplitudes of waves A and B) was such that

$$Q \geq \min(Q_A, Q_B,), \tag{29}$$

where Q_A and Q_B depend on the orientation of the wave vectors and are given by Eqs. (24) and (24) (see Fig. 1).

This prediction was confirmed by bidimensional direct numerical simulations of the Navier–Stokes equations under the Boussinesq approximation, the initial condition being the superposition of two monochromatic waves with no vertical mean shear. In the sub-critical case, the mean current was approximately time-periodic with a slightly increasing mean value. This slow drift may be due to a weak non-linearity or to the effect of viscosity which dissipates the large-scale growing mode more slowly than the wavy motions. In the over-critical case, nonlinear transfers were observed from the waves to the mean flow and the flow was finally dominated by the mean current. The effect of wave instability was also investigated by switching off the retroaction of the mean flow on the waves in the over-critical simulation. We found that the waves became unstable but did not produce any significant vertical mean shear. This allowed us to conclude that the interaction between the waves and the induced mean flow was the dominant mechanism.

It is likely that such a wave–wave–mean flow interaction can partly explain the presence of strong vertical shear modes in geophysical flows, such as stratified wakes of obstacles or moving bodies in oceans and atmospheres. It could also be involved in the acceleration of horizontal mean currents by stratified turbulence as observed in DNS of stratified turbulent shear flows (see Galmiche et al., 1997, 1998, 1999). To get closer to realistic situations, our predictions might be improved by taking the effect of the Earth rotation into consideration.

This mechanism may also help to understand the production of intense horizontal currents by the interaction between a breaking wave and the induced secondary modes as observed by Lombard (1994).

Acknowledgements

This study was sponsored by the DRET and computing resources were supplied by the IDRIS.

References

Booker, J.R., Bretherton, F.P., 1967. The critical layer for internal gravity waves in a shear flow. J. Fluid Mech. 27, 513–539, Part 3.

Frisch, U., Su She, Z., Thual, O., 1986. Viscoelastic behaviour of cellular solutions to the Kuramoto–Sivashinsky model. J. Fluid Mech. 168, 221–240.

Galmiche, M., Thual, O., Bonneton, P., 1997. Direct numerical simulation of turbulence in a stably stratified fluid and wave–shear interaction. J. Appl. Sci. Res., in press.

Galmiche, M., Thual, O., Bonneton, P., 1998. Acceleration of horizontal mean currents in DNS of turbulent shear flows. In: Proc. ETC-7, Advances in Turbulence. Kluwer Academic Publishers, pp. 423–424.

Galmiche, M., Thual, O., Bonneton, P., 1999. Acceleration of a horizontal mean current by turbulence in a density-stratified fluid. Phys. Fluids (submitted).

Garrett, C., Munk, W., 1979. Internal Waves in the Ocean. In: Van Dyke, M. (Eds.), Annual Review of Fluid Mechanics. Annual Reviews 11, 339–369.

Koop, C.G., 1981. A preliminary investigation of the interaction of internal gravity waves with a steady shearing motion. J. Fluid Mech. 113, 347–386.

Lelong, M.P., Riley, J.J., 1991. Internal wave-vortical mode interactions in strongly stratified flows. J. Fluid Mech. 232, 1–19.

Lombard, P.N., 1994. The stability of Finite Amplitude Internal Gravity Waves. PhD Thesis, Univ. of Washington.

Martin, S., Simmons, W., Wunsch, C., 1972. The excitation of resonant triads by single internal waves. J. Fluid Mech. 53, 17–44, part 1.

McComas, C.H., Bretherton, F.P., 1977. Resonant interaction of oceanic internal waves. J. Geophys. Res. 82 (9), 1397–1412.

Phillips, O.M., 1968. The interaction trapping of internal gravity waves. J. Fluid Mech. 34, 407–416, part 2.

Teoh, S.G., Ivey, G.N., Imberger, J., 1997. Laboratory study of the interaction between two internal wave rays. J. Fluid Mech. 336, 91–122.

Thual, O., 1992. Zero-Prandtl number convection. J. Fluid Mech. 240, 229–258.

Winters, K.B., D'Asaro, E.A., 1994. Three-dimensional wave instability near a critical level. J. Fluid Mech. 272, 255–284.